The Aeronautical Journal (2024), 1–16
doi:10.1017/aer.2024.99

RESEARCH ARTICLE

Experimental research on detonation initiation and transition in millimeter-scale planar combustion chambers

Y. Gao , Y. Yan , Z. Wang , B. Yang and H. Hu

National Key Laboratory of Aerospace Liquid Propulsion, Xi'an Aerospace Propulsion Institute, Xi'an, China
Corresponding author: Z. Wang; Email: wangzhichengnwpu@163.com

Received: 11 December 2023; **Revised:** 28 June 2024; **Accepted:** 10 July 2024

Keywords: experiment; millimeter gap; flame acceleration; detonation transition; flame visualisation

Abstract

To investigate the flame acceleration to detonation in 2.0 and 0.5 mm planar glass combustion chambers, the experiments have been conducted utilising ethylene/oxygen mixtures at atmospheric pressure and temperature. The high-speed camera has been used to record the revolution of flame front and pressure inside the combustion chamber. Different equivalence ratios and ignition locations have been considered in the experiments. The results show that the detonation pressure in the 2 mm thick chamber is nearly three times of Chapman-Jouguet pressure, while detonation pressure in the 0.5 mm thick chamber is only 45.7% of the Chapman-Jouguet value at the stoichiometric mixture. This phenomenon is attributed to the larger pressure loss in the thinner chamber during the detonation propagation. As the value of equivalence ratio is 2.2, the detonation cannot be produced in the 2 mm thick chamber, while the detonation can be generated successfully in the 0.5 mm thick chamber. This phenomenon indicates that the deflagration is easily to be accelerated and transformed into the detonation, due to a larger wall friction and reflection. Besides, the micro-obstacle has been added into the combustor can shorten the detonation transition time and reduces the distance of the detonation transition.

Nomenclature

A	throat area of the sonic nozzle
C_d	the flow coefficient
K	the gas constant
p^*	the gas inlet pressure
$p_{C\text{-}J}$	the theoretical Chapman-Jouguet pressure
T^*	the gas inlet temperature
t	operation time
$v_{C\text{-}J}$	the theoretical Chapman-Jouguet velocity
v_i	the propagation velocity of detonations
L	the distance of the flame front between two adjacent frames
$\triangle t$	the time interval between two adjacent frames
σ_{vi}	the error of the propagation velocity
σ_L	the error of the length of the pixel points
σ_{vi}	the error of the propagation velocity

1.0 Introduction

Micro-scale or small-scale combustion has been paid more attention, as it can be developed for not only engineering purposes but also as an effective approach to understand the fundamentals of combustion. Chemical reactions can propagate through the explosive mixtures at supersonic speeds as a detonation

wave: a compression shock with an abrupt increase in the thermodynamic state, initiating chemical reactions that turn the reactants into products [1]. This detonation process results in a lower entropy gain than deflagration and, therefore, a detonation-based cycle has a higher thermodynamic efficiency than the traditional constant-pressure Brayton cycle. The detonation wave has been regarded as an alternative to the conventional propulsion systems in aeronautical engines, even within the scope of micro-combustion. Besides, it is important to conduct the research of the detonation initiation and transition processes for ensuring the engineering safety.

The different near-limit detonation phenomena, which are highly unstable and easily quenched and transformed into the deflagration, have been found and named, such as low-velocity detonation, spinning detonation, galloping detonation and stuttering detonation. The intrinsic feature of the near-limit detonation combustion has not been fully clarified. This is caused by the complexity of detonation combustion, especially at near-limit conditions. Roughly, combustion wave can be classified into deflagration and detonation according to its propagation velocity. At some conditions, deflagration can accelerate to fast deflagration and even detonation. Detonation velocity will decrease when it is propagated into a small tube or rough walled tubes. In some cases, detonation can transform into low-velocity detonation, which is also known as quasi-detonation. Flame acceleration and detonation transition in combustors with dimensions approaching the flame thickness have drawn numerous research interests in recent years and most research has focused on the deflagration-to-detonation transition (DDT) in small tubes and channels. The unstable detonation appears accompanied with large velocity oscillation and the averaged velocity 10%–30% lower than theoretical Chapman-Jouguet (C-J) velocity. If initial pressure is further decreased, the fast deflagration mode with velocity about 50% of the C-J value is observed.

Experiments have been performed by Li et al. [2] to achieve a strong overdriven detonation wave in the weaker mixture via the DDT process. The results show that a rarefaction effect must be generated to ensure that there is no overestimate of the post-transmission wave properties when the incident detonation wave is overdriven. The near C-J state of the incident wave leads to a transmitted shock wave, and then the transition to the overdriven detonation wave occurs downstream. Flame propagation in capillary tubes with smooth circular cross-sections and diameters of 0.5, 1.0 and 2.0 mm have been investigated [3]. Flames have been found to propagate and accelerate to detonation in all three tube diameters. The transition of detonation in micro tubes have been observed for the first time. Three types of flame propagation modes have been observed in the 0.5 mm tube with spark ignition: (a) successful acceleration to C-J detonation velocity, (b) C-J detonation followed by failure and (c) acceleration to a constant speed below the C-J speed. Boundary layer effect, turbulence, autoignition of pre-compressed and preheated unburned mixture have been discussed for flame acceleration process. Spinning detonations have been studied to reveal characteristics of spinning modes by using three-dimensional simulations with a detailed chemical reaction model [4]. The numerical result shows that the spinning detonation in the circular tube is composed of the transverse detonation, the Mach leg and whiskers as well as the long pressure trail extending downstream of the tube. Detonation wave structure of H_2/O_2 mixture in the narrow channel has been also modeled by Bondar et al. [5]. Detonation velocities and soot patterns of spinning detonation in glass tubes of 3, 6 and 10 mm diameters have been studied by Kitano et al. [6], in order to elucidate the limits of detonation. It is found that transition from a multi-head detonation to a single-head spinning detonation can happen at a certain initial pressure and velocity deficit is about 5%. The dominant factor for the velocity deficit results from the heat and momentum loss and the limit of detonation may be governed by those loss terms. Detonations of stoichiometric ethane/oxygen mixture in micro capillary tubes with inner diameters of 0.13, 0.25, 0.50 and 1.0 mm have been studied [7]. The explosion propagation velocities are always higher than the supersonic values or no detonation propagation has been occurred. Subsonic velocities have been never observed. For all capillary diameters, the propagation velocities of detonations are lower than the C-J value.

Detonation limits in small diameter tubes (1.8–9.5 mm) have been investigated to further the understanding of the near-limit detonation phenomenon [8]. They state that boundaries generate heat and momentum losses, and these losses can cause detonation velocity deficits and eventually failure in small

https://doi.org/10.1017/aer.2024.99 Published online by Cambridge University Press

tubes. For most gaseous combustible mixtures, instabilities provide an essential mechanism for detonation propagation. The propagation phenomenon is generally unsteady and very complex near the limit conditions. They also have found that detonation is slightly overdriven upon exiting the steel section into the smaller diameter test section. Detonation velocity deficits in narrow channels have been experimentally studied with a focus on velocity deficits and variation in cell widths [9]. It is found that a combination of the calculated velocity deficit and the number of cells in a channel contributes to the prediction of propagation limits of detonations. The turbulence-detonation interaction has been considered by Massa et al. [10]. The fundamental difference between the shock and detonation problems is the presence of a self-excited unstable region in the detonation front. Their results indicate that propagation in rough pipes leads to incomplete combustion. Wu et al. [11] experimentally have researched detonation transmission through a planar sudden expansion in a narrow channel. Visualisations show that the detonation waves have been extinguished and accompanied by an abrupt decrease of propagating velocities after passing through the sudden expansion. However, re-acceleration of the reaction front and re-initiation of the detonation wave have been observed downstream in the expanded receptor section. Velocity characterisation shows that steady propagating speed of the detonation wave is about 100 m/s higher in receptor section than in the initiator section. The classic DDT limits obtained in flame acceleration and DDT experiments are governed predominantly by the detonation propagation mechanism. The detonation initiation process that cannot occur locally in the obstacle section outside the limits.

Minimum tube diameters and detonation limits in tubes have been researched [12, 13]. They have stated that measured minimum tube diameters can be reasonably estimated on the basis of the $\lambda/3$ rule over a wide range of conditions. They also have found that the detonation velocity, in rough tubes, is generally much lower than that in smooth tubes. However, the detonation limits in rough tubes are found to be wider than for a smooth tube. Smoked foil records show that the detonation front has a cellular structure in the core of the rough tube, corresponding to the usual cellular structure due to instability of the detonation. They have explained that the wall roughness tends to facilitate the self-sustained propagation of detonation waves. The detonation initiation and propagation characteristics in millimeter tubes or narrow channels have been studied [14–16]. The heat loss has a great influence on the formation of precursor shock wave and affects the detonation forming process. In the ethylene-oxygen mixture, heat loss effect is not significant because of its high reactivity. Compared with large-scale tubes, it is believed that the boundary layer plays an important role in the flame acceleration process in narrow gaps. Acceleration and transition to detonation in 260 and 120 μm gaps have been experimentally studied [17, 18]. Detonation can be generated in the thin gaps and eventually propagates at near C-J velocities. Flame acceleration and detonation initiation in channel combustors with width of 1–4 mm, height of 10–30 mm and length of 1,220 mm have been experimentally studied [19]. They have found that the detonation transition distance is strongly dependent on the initial pressure and the gap size. The flame development rule in millimeter narrow gap and circle tube is obviously different at the same initial pressure.

These studies have suggested that the flame acceleration and transition into the detonation in small tubes have been extensively studied. However, fewer studies have been conducted to reveal the detonation wave initiation process and propagation characteristics in other shaped channels, such as the planar gap combustor. It is very important to study the propagation characteristics of detonation waves in various structures for engineering safety and engine propulsion. Different phenomena of detonation wave initiation and propagation in different structures are still not completely clarified from experiments and need to be further evaluated. As a result, the purpose of the present study is to reveal the ignition, flame acceleration and detonation initiation in planar gap combustors.

2.0 Experimental method

An annular Teflon shim is placed between a circular metal base and a circular Plexiglas to create a planar gap in a circular shape with a thickness of millimeters. The inner diameter of the shim is 300

https://doi.org/10.1017/aer.2024.99 Published online by Cambridge University Press

mm, which means that the diameter of circular gap is 300 mm. The gap thickness can be adjusted by changing the shim with different thickness. In the present study, two shims have been used to create gaps in thickness of 0.5 and 2 mm and the schematic of the micro-chamber structure is shown in Fig. 1. The 1 mm diameter hole is in the centre of the metal base, which is inlet for combustible mixture. Four holes with the diameter of 2 mm are placed circumferentially in the metal base and near the gap edge, which serve as the outlets of the micro-chamber. There are two ignition locations which are 20 and 60 mm away from the centre, respectively. The ignition point which 20 mm away from the centre was used in all tests, except for the case 5. The energy released of the spark is about 6mJ. The piezoresistive pressure transducer (Kistler 6054BRU20) has been installed in the metal base to record combustion pressure, and the measuring face of the pressure transducer is at the same plane as the metal base surface in the chamber. A micro-obstacle has been installed into the micro-chamber which is away from 60 mm from the left side of the micro-combustor centre in the case 6, and no obstacle has been installed in other cases, as shown in Fig. 1(d). The micro-obstacle's diameter is 14 mm and the gap thickness is 0.5 mm.

The experimental system setup is shown in Fig. 2. The fuel and oxidiser are ethylene and oxygen, respectively. Sonic nozzles have been used to control mass flow rates of fuel and oxidiser, allowing to alter equivalence ratios by adjusting the supply pressures before the sonic nozzles. Fuel and oxidiser have been premixed in a mixer before entering the micro-combustor. The static pressures upstream and downstream sonic nozzles have been recorded by low-speed sensors (DaCY420) with sampling rate 1,000Hz and the accuracy is 1%. The piezoresistive pressure transducer has been utilised to measure the combustion pressure with the range 0–30 MPa and the measuring accuracy is 0.5%. The high frequency pressure signals have been recorded by a LMS acquisition device. A signal generator (DG535) has been used to trigger the ignition spark and high-speed CCD camera (Phantom v12.1) synchronously. The frame recording frequency of the high-speed camera has been preset the ranges from 40,000 to 67,065 fps, which the frequency is enough to capture the detonation wave. The exposure time is fixed at 5 μs.

The experiment steps as following: at first, the micro-chamber has been filled with fuel and oxidiser. Then, the filling period has lasted about seven seconds as shown in Fig. 3, and the mixture inside the chamber has been ignited by the spark. During the filling process, two filling modes have existed, including supersonic filling and subsonic filling, which is caused by the properties of the valves in the supply pipes. The valves cannot shut off immediately when receiving closing signal because of their mechanical inertia. The supersonic filling period has lasted more than four seconds to ensure that the air inside the micro-chamber is entirely replaced by the premixed mixture. When the pressures of the sonic nozzle upstream and downstream have been acquired, the mass flow rates of fuel and oxidiser can be calculated using aerodynamic formulas in Equation (2), where K_{H2} is 0.0106 and K_{O2} is 0.0425.

$$q_m = C_d K \frac{p^*}{\sqrt{T^*}} A \tag{1}$$

3.0 Results and discussions

In the present study, the equivalence ratio, chamber thickness and ignition position have been varied and the parameters of different experimental cases are shown in Table 1. The theoretical C-J values at different equivalence ratios have been calculated through CEA [20].

3.1 Detonation transition at the stoichiometric equivalence ratio

As shown in Fig. 4, the flame front evolution inside a 2 mm thick planar combustor has been captured by the high-speed CCD at stoichiometric equivalence ratio. The recording rate is 41,025 fps and exposure time is 5 μs. At the beginning stage (0–73 μs), the flame propagation velocity is very slow and it's

https://doi.org/10.1017/aer.2024.99 Published online by Cambridge University Press

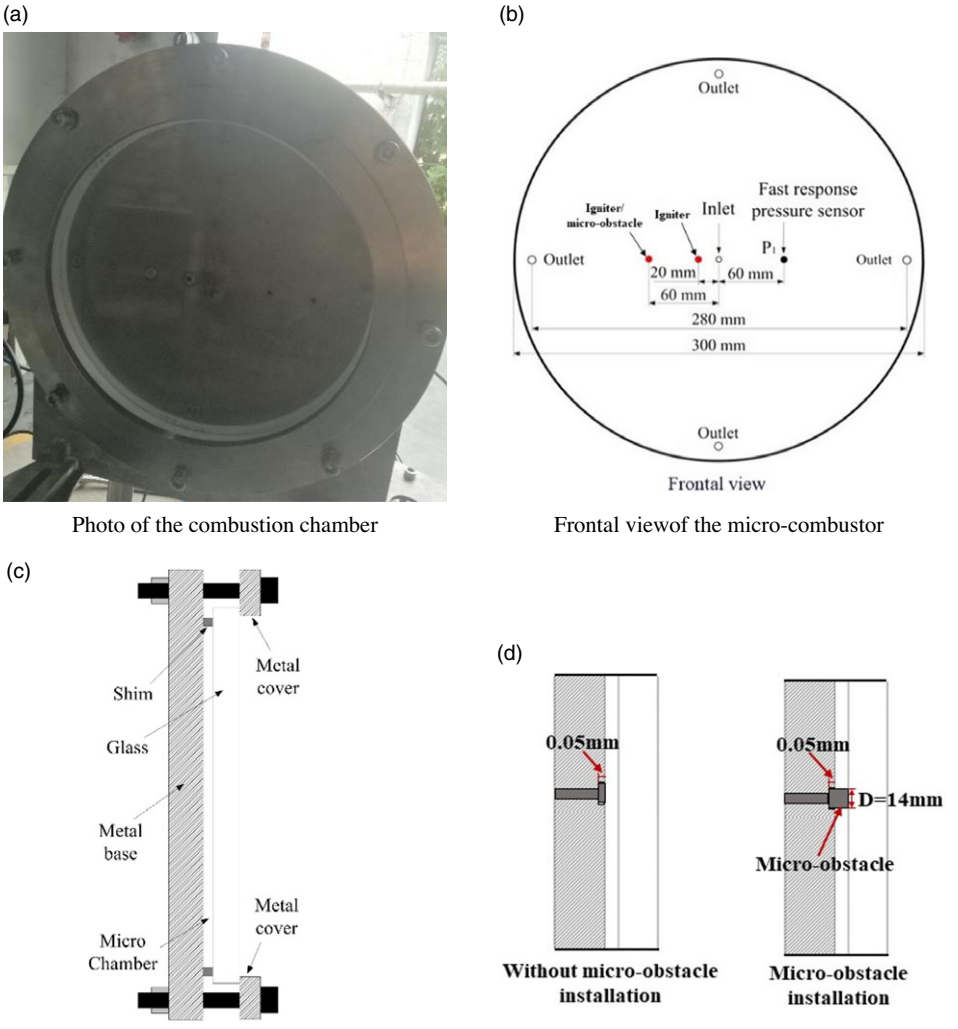

Figure 1. *Schematic of the micro-chamber.*

difficult to calculate the averaged propagating velocity. Then from 97 to 170 μs, the flame front grows as a circle. The flame front starts to distort in the left side at 195 μs and finally a very strong combustion is generated when the flame reaches the left edge at 365 μs.

The propagation velocity of the detonation has been calculated from the frame front captured by high-speed visualisations, as illustrated in Equation (2). Besides, the error of the propagation velocity of the detonation has been calculated by Equation (3), where σ_L is the error of the length of the pixel points, which is around 1 mm.

$$v_i = L/\Delta t \tag{2}$$

$$\frac{\sigma_{vi}}{v_i} = \sqrt{\left(\frac{\sigma_L}{L}\right)^2 + \left(\frac{\sigma_{\Delta t}}{\Delta t}\right)^2} \tag{3}$$

https://doi.org/10.1017/aer.2024.99 Published online by Cambridge University Press

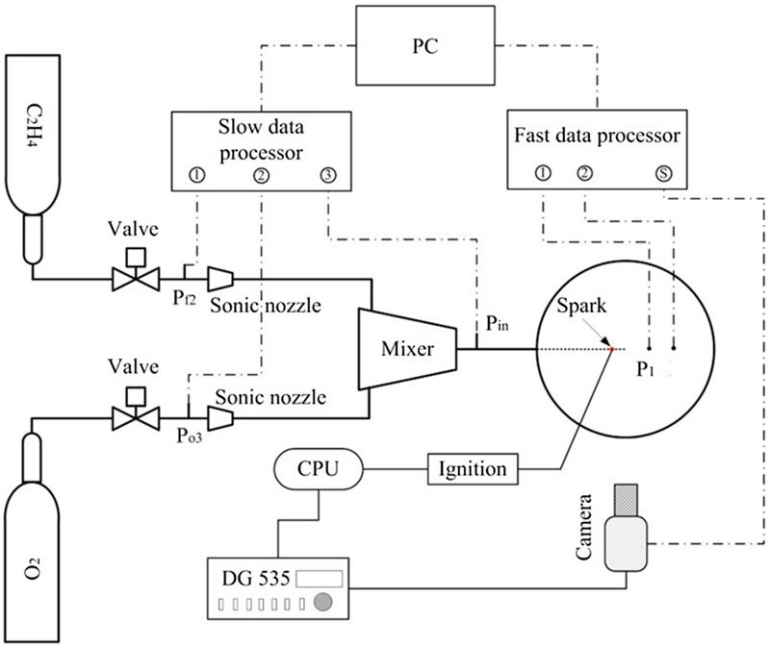

Figure 2. *Schematic of experimental apparatus.*

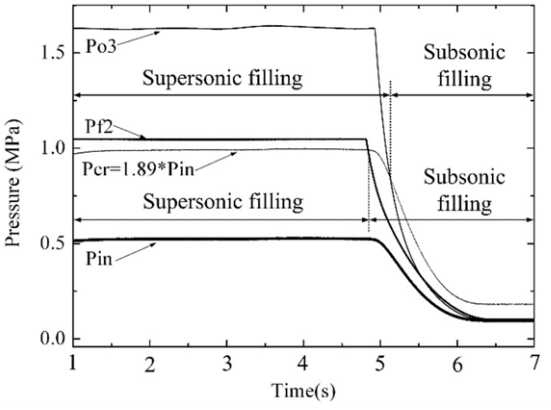

Figure 3. *Supplying pressure history during filling period.*

Averaged Cpropagating velocity can be calculated by tracking the flame front. The flame front and velocities at the left and right sides have been calculated as shown in Fig. 5. Besides, the pressure history measured from piezoresistive pressure transducers is shown in Fig. 6. At the early stage before 195 μs, the flame propagation velocities at both sides are nearly the same and after that velocity of the left side grows a little faster, which might be caused by the second ignition port, which is 60 mm away from the centre. The velocity increases sharply after 316 μs, because the flame front at left side is approaching more closer to the wall and finally the velocity at left side is about 1,526 m/s at 365 μs. It indicates that wall obstacle is helpful for the flame acceleration inside the planar combustor. In this case, the C-J detonation pressure is 3.28 MPa and C-J detonation velocity is 2,373 m/s. As shown in Fig. 5, the velocity obtained from this case is obviously lower than the C-J velocity. In Fig. 6, it is t=330 μs after

https://doi.org/10.1017/aer.2024.99 Published online by Cambridge University Press

Table 1. *Parameters of selected experiment cases*

Case number	Equivalence ratio	Chamber thickness (mm)	C-J values		Note
			Pressure (MPa)	Velocity (m/s)	
1	1.0	2.0	3.28	2,372.8	/
2	1.0	0.5	3.28	2,372.8	/
3	2.2	2.0	4.06	2,697.6	/
4	2.2	0.5	4.06	2,697.6	/
5	1.0	0.5	3.28	2,372.8	Ignited near wall
6	1.0	0.5	3.28	2,372.8	Obstacle inside

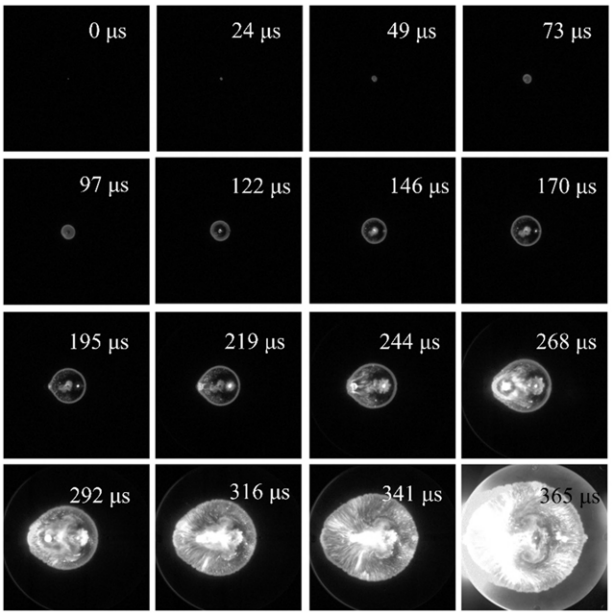

Figure 4. *High-speed visualisation of the flame propagation (case 1).*

ignition that the pressure sensor p_1 capture the first pressure peak at 0.86 MPa, which is much lower than the C-J pressure value. As illustrated in Fig. 5, the peak pressure is almost three times of C-J pressure at 498 μs. The pressure peak measured from pressure sensor p_1 indicates that a detonation wave has been produced in the detonation tube and successfully propagates inside the test section. The initiation process of the detonation wave is as follows, a combustion wave propagates with the type of the deflagrations via the diffusion of heat and mass from the flame zone in the initial stage [1]. The flame front gradually becomes unstable and a train of weak compression waves can be observed in front of the propagating flame. The deflagration tends to accelerate to the maximum velocity of the half C-J detonation speed subsequent around 340ms, and the spontaneous onset of detonation would take place.

In the case 2, the combustor thickness varies to 0.5 mm, and the equivalence ratio remains the same value of the case 1. The combustion happens much faster in a smaller area with the higher frame rate was selected here, which is 67,065 fps. The evolution of flame structure, flame front propagation velocity and pressure history are shown in Figs. 7, 8 and 9, respectively. From 0 to 180 μs, the flame front grows as a circle with the propagation velocity around 500 m/s. Two hotspots with high brightness appear at the upper edge and lower edge of the flame front at 195 μs, and then the strong explosions happen near these hotspots. The propagation velocity accelerates to 2,500 m/s and is higher than the C-J velocity, which indicates that the detonation wave has been generated. However, the peak pressure is around 1.5

https://doi.org/10.1017/aer.2024.99 Published online by Cambridge University Press

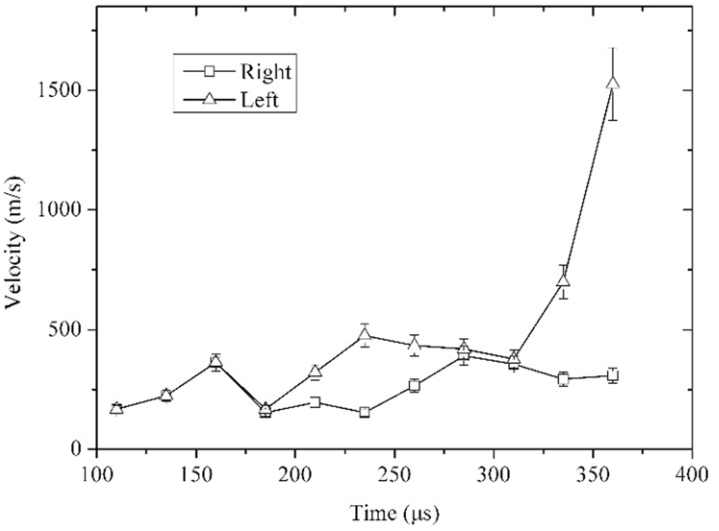

Figure 5. *Averaged velocity of flame front (case 1).*

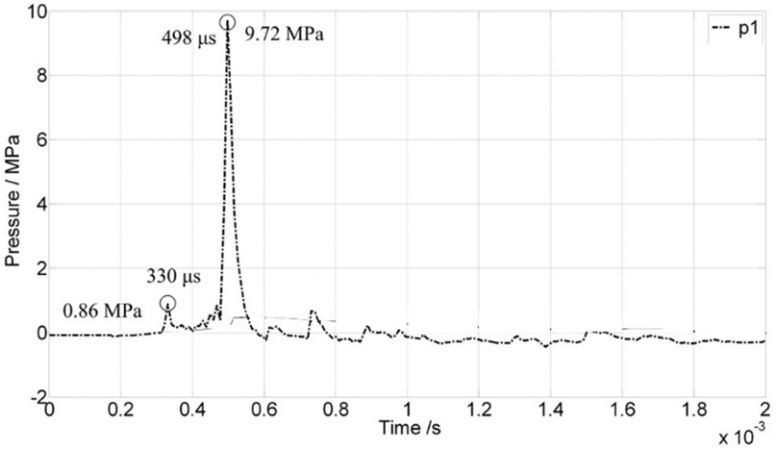

Figure 6. *Pressure history inside micro-chamber (case 1).*

MPa, as shown in Fig. 9, which is lower than the C-J detonation pressure (45.7% of C-J pressure). This phenomenon indicates that the detonation in a 0.5 mm thick gap is quite different from that in a 2 mm thick gap. Although the evolution of flame from deflagration to detonation is much faster in a thinner chamber, the detonation pressure is much lower. In the thinner chamber, the flame is easily becoming turbulent and forming a so-called tulip-shaped flame, which the combustion wave spreads faster near the wall. The flame area of the tulip-shaped flame is obviously increase and the second flame acceleration happens in the boundary region, which increases not only the displacement flow velocity ahead of the flame but also the generation of pressure waves associated with the increase in burning rate. The propagation velocity of the deflagration tends to reach values of the half the C-J detonation speed faster. The pressure wave reflects from the top and bottom wall of the channel and, therefore, the local explosion centres is generated easily. Moreover, the explosion centre propagates forward and transforms into an overdriven detonation, which the propagation speed of detonation wave is higher than

https://doi.org/10.1017/aer.2024.99 Published online by Cambridge University Press

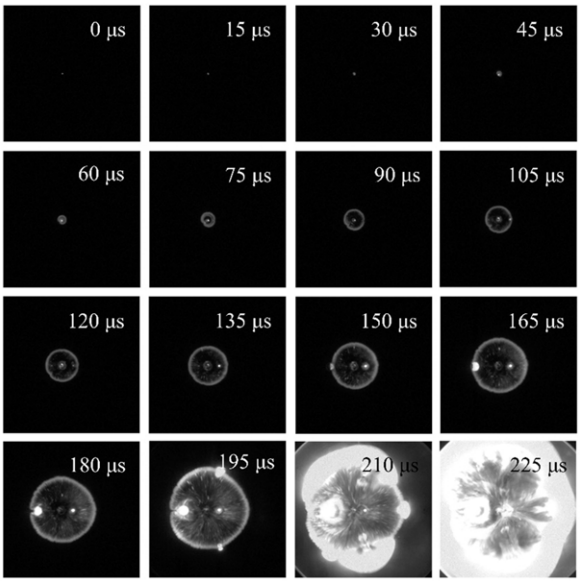

Figure 7. *High-speed visualisation of the flame propagation (case 2).*

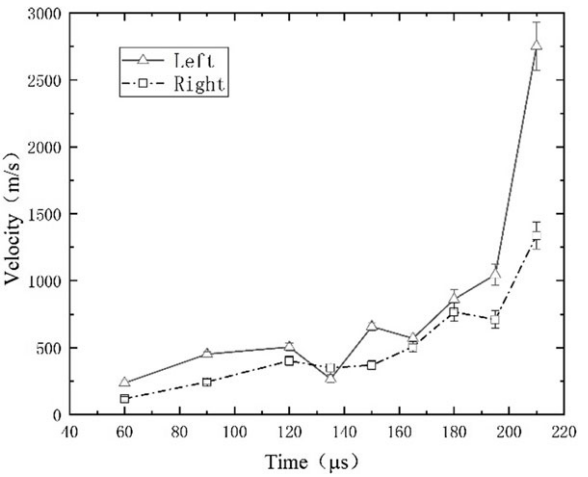

Figure 8. *Averaged propagation velocity of flame front (case 2).*

the theoretical value as illustrate in Fig. 8. However, the loss caused by the boundary layer in a thinner chamber also reduces the peak pressure of the detonation wave.

3.2 Detonation transition at the fuel rich cases

The equivalence ratio increases to 2.2 in the case 3. Fig. 10 shows that the propagation velocity of the combustion wave is much slower in the thick combustor, compared with the stoichiometric case. After ignition around 2,219 μs, a very weak flame front is visible. At the first row in Fig. 10, the flame front grows as nearly a circle if we neglect some small local protrusions. When the flame propagates further outward, the flame front at the left top area begins to distort. This indicates that

https://doi.org/10.1017/aer.2024.99 Published online by Cambridge University Press

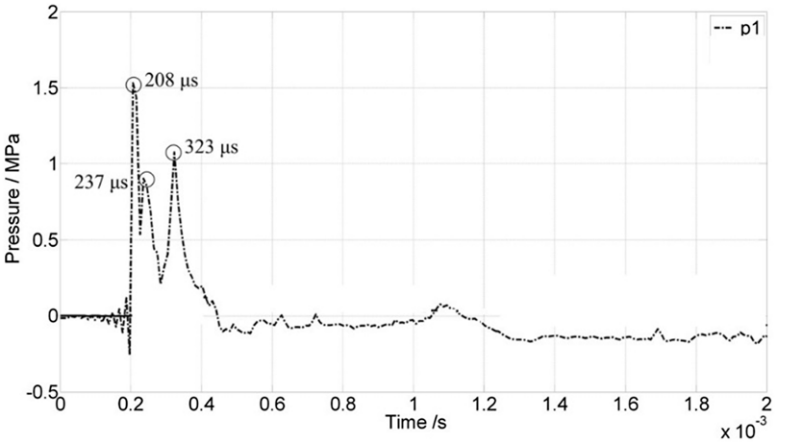

Figure 9. *Pressure history inside the micro-chamber (case 2).*

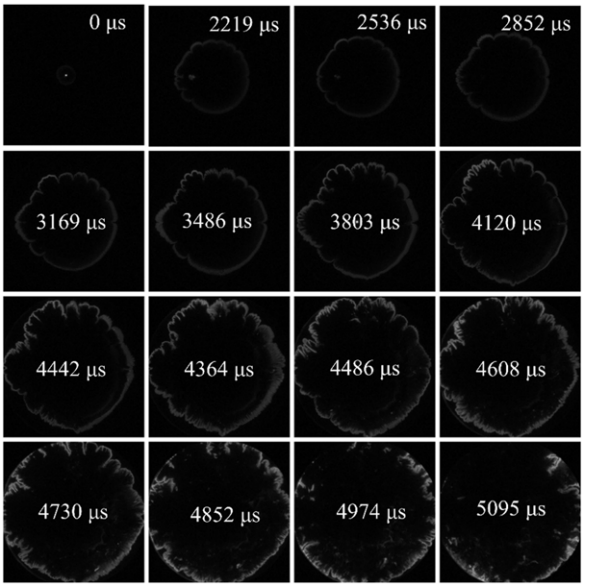

Figure 10. *High-speed visualisation of the flame propagating process (case 3).*

combustion rate difference is getting larger and larger at different area. However, the flame propagation velocity is too slow to transfer to detonation. If the small flame wrinkles have been neglected, the global time-averaged flame propagation velocity is about 31 m/s. It is turbulent deflagration combustion. In this case, the combustion rate is very slow and the peak pressure of the combustion wave is lower than the C-I pressure value, as illustrated in Fig. 11, which means that the detonation cannot be produced.

As the equivalence ratio is fixed at 2.2 in the case 4, the flame evolution in Fig. 12 shows a more rapidly propagated flame compared with that shown in Fig. 10. The averaged propagation velocity of the flame front is shown in Fig. 13 and the peak pressure of the combustion wave is illustrated in Fig. 14. From ignition to 626 μs, the average flame propagation velocity is very slow. After 626 μs, the flame starts to accelerate and wrinkled flame appears. But the flame spreading propagation velocity is

https://doi.org/10.1017/aer.2024.99 Published online by Cambridge University Press

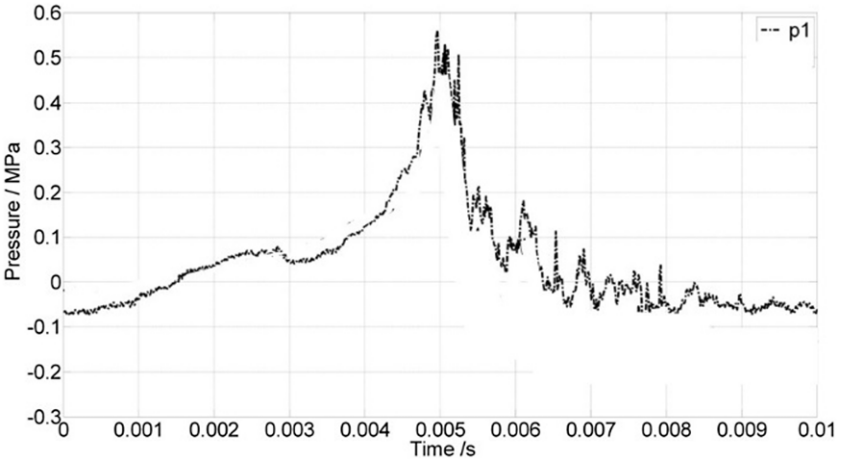

Figure 11. *Pressure history inside the micro-chamber (case 3).*

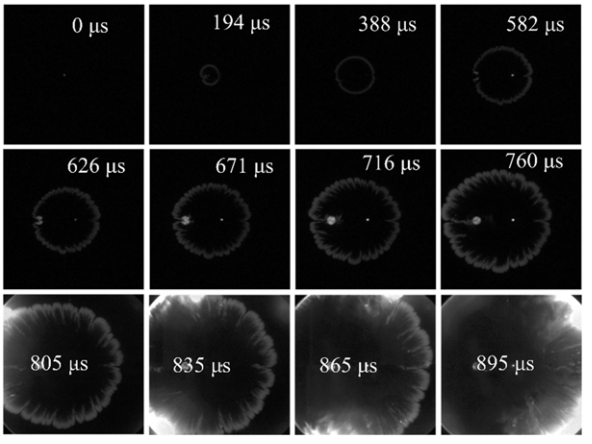

Figure 12. *High-speed visualisation of the flame propagation (case 4).*

obviously lower than the C-J velocity, thus it is still a fast deflagration flame. The left flame front reaches the outlet wall and the collision generates a local explosion at 805 μs, which the bright area is shown in the frame. Then this hotspot moves very fast along the outer ring of the circular chamber because the combustible mixture in the centre of the chamber has been consumed by the fast deflagration. The propagating velocity is more than 2,800 m/s (104% of C-J velocity), indicating that a detonation wave is generated inside the chamber.

In short, the detonation is more easily to happen inside the thinner chamber and the transition time from deflagration to detonation is shorter. Thinner gap means larger boundary loss, and more heat loss, which are negative for detonation transition. However, flow resistance in the thinner chamber is beneficial for flame acceleration because it can promote the reflection from the top and bottom walls and enhance the turbulence of the flow field. The combustion wave spreads faster near the wall. Therefore, the detonation is more easily produced in the thinner combustor. Another interesting phenomenon is that the propagation velocity of the detonation is close to C-J value while the peak pressure is much lower than C-J value. In the 2 mm thick chamber, a higher pressure value can also be recorded which means the little effect of the fraction loss caused by the boundary walls on the peak pressure of the detonation.

https://doi.org/10.1017/aer.2024.99 Published online by Cambridge University Press

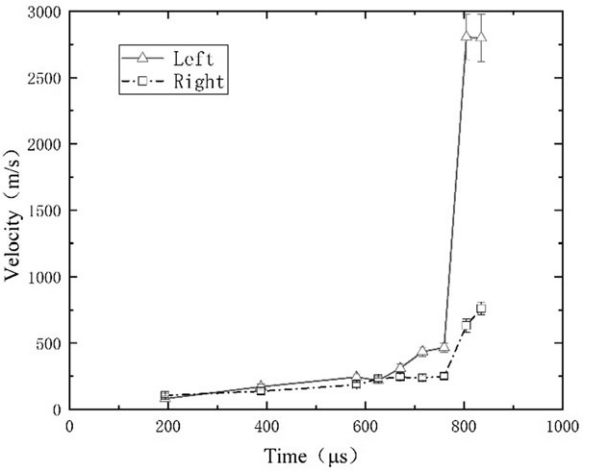

Figure 13. *Averaged propagation velocity of flame front (case 4).*

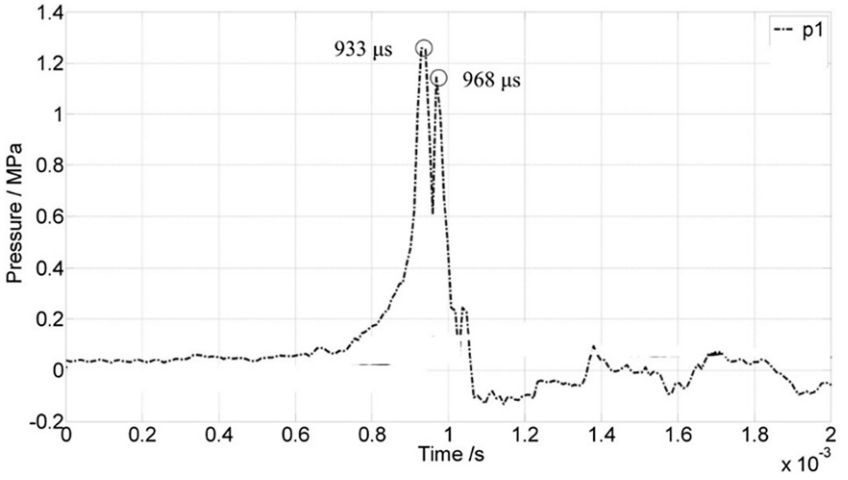

Figure 14. *Pressure history inside the micro-chamber (case 4).*

In a thinner chamber, the influence of the boundary loss on the peak pressure of the detonation wave is more prominent.

3.3 Effect of the wall reflection on detonation transition

In the case 5, the ignition location has been changed to 60 mm away from the combustor centre and effect of the wall reflection on the flame acceleration has been evaluated. The gap thickness is 0.5 mm, and the equivalence ratio is 1.0 in this case. As shown in Fig. 15, the flame evolution shows that the flame grows as a circle before it reaches the wall. As the flame front arrives at the boundary wall of the circle, a very strong explosion forms with an obvious highlight area. Two detonation fronts can be seen at 170 μs, which travel very fast towards unburned area and have merged into one wave finally. The detonation occurs about 64 μs earlier than that in the case 2.

As shown in Fig. 16, the flame acceleration processes, in the case 2 and the case 5, have been compared and the detonation is generated earlier in the case 5. This phenomenon can be explained that the

https://doi.org/10.1017/aer.2024.99 Published online by Cambridge University Press

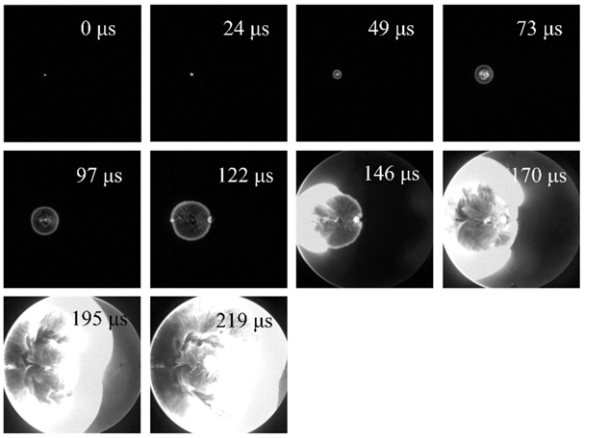

Figure 15. *High-speed visualisation of the flame propagation (case 5).*

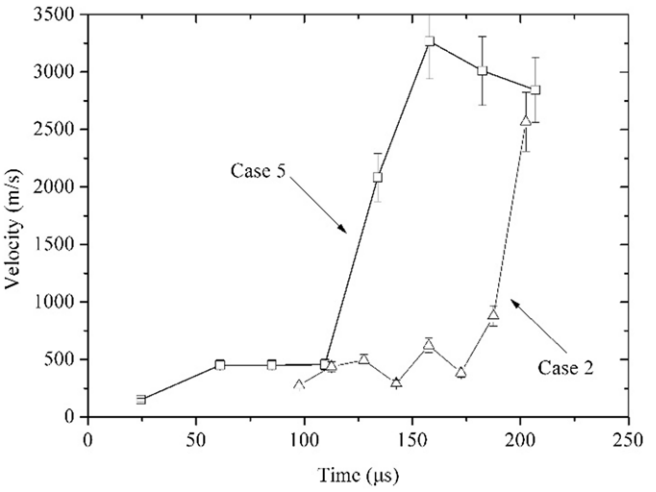

Figure 16. *Averaged propagation velocity of flame front (case 2 and case 5).*

expansion wave generated from the deflagration reaches the boundary wall of the circle and the reflected wave would be formed. This reflected wave would couple with the combustion wave and strengthen the combustion reaction. Thus, the local explosion hotspot more easily occurs and plays an active role to produce the detonation. In this case, the detonation velocity and detonation pressure are higher than that in the case 2, as shown in Figs. 16 and 17. This means that wall reflection can produce a stronger detonation earlier if the ignition port is closer to the wall.

3.4 Effect of the micro-obstacle on detonation transition

In the case 6, all the geometry setup is the same with that in the case 2, except that the micro-obstacle has been installed into the combustor. The obstacle has been utilised to investigate the effect of the micro-obstacle on the flame acceleration process. The gap thickness is 0.5 mm and the equivalence ratio is 1.0. In Fig. 18, the flame front passed the obstacle, between time 150 and 175 μs, and local explosion happens. Averaged propagating velocity during this period is about 2,737 m/s, which is 115% of the C-J

https://doi.org/10.1017/aer.2024.99 Published online by Cambridge University Press

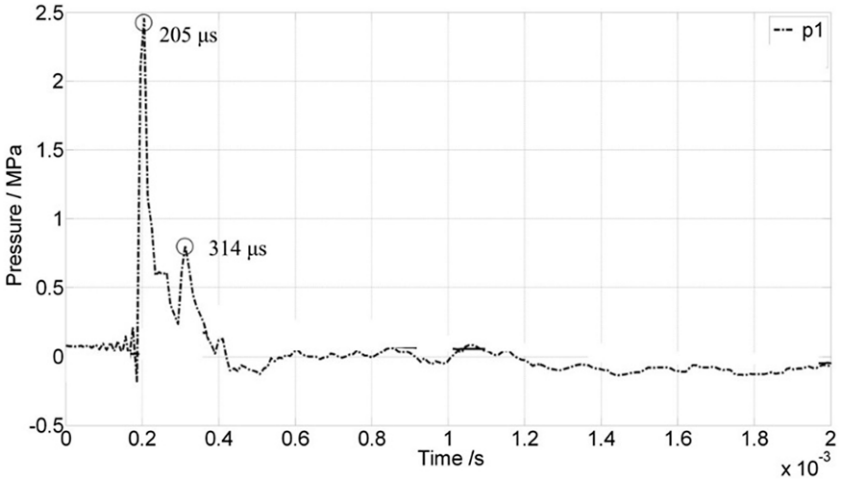

Figure 17. *Pressure history inside the micro-chamber (case 5).*

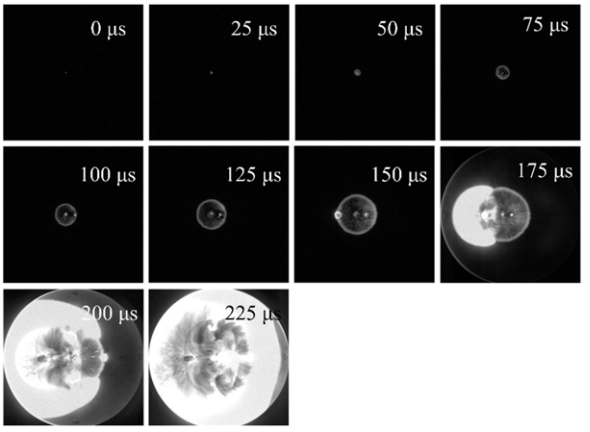

Figure 18. *High-speed visualisation of the flame propagation (case 6).*

value and indicates that the transition to detonation completed in this period. The flame acceleration to detonation is faster and pressure peak, as shown in Fig. 19, is larger than that in the case 2. It can be obtained that an obstacle added in the micro-chamber is very useful for flame transition into detonation. As the flame front passes through the obstacle, the flame surface would rapidly increase and results in the further increase of the flow velocity. Besides, the turbulence of the flow field would increase behind the obstacle and the local burning rate would also increase. The flame further accelerates and renders the compression wave stronger. Therefore, the hotspots can be easily generated and shorten the DDT distance.

4.0 Conclusions

In order to clarify the detonation initiation and transition in the millimeter-scale planar chambers, the thickness of combustor, equivalence ratios, the ignition location and the obstacle have been varied in this study. Compared with the results of the 2 mm thick chamber, the flame more easily accelerates and transforms into the detonation with a higher propagation speed. However, the loss caused by the

https://doi.org/10.1017/aer.2024.99 Published online by Cambridge University Press

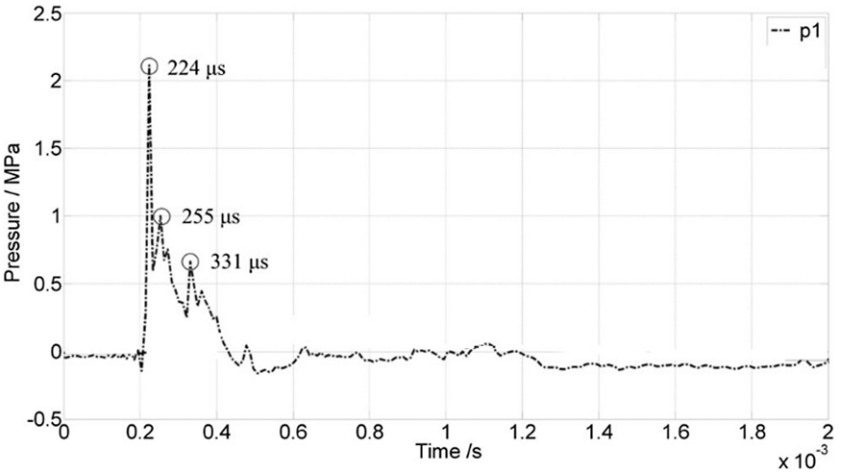

Figure 19. *Pressure history inside the micro-chamber (case 6).*

boundary layer in a thinner chamber also reduces the peak pressure of the detonation wave. At the fuel rich cases, detonation cannot be triggered in the chamber with the thickness of 2 mm, but it still can be occurred in the 0.5 mm chamber. This result indicates that the detonation is easier to trigger in a thinner chamber. The wall reflection plays a very important role on the detonation transition in this millimeter planar chamber. The weak expansion wave ahead of the flame front reaches the boundary wall of the circle and the reflected wave is formed. This reflected wave would couple with the combustion wave and the local explosion hotspot more easily occurs which transition to detonation is faster. The micro-obstacle added in the micro-chamber is very useful for flame transition into detonation, due to the local burning rate and turbulence of the flow field would increase behind the obstacle and the hotspots can be easily generated to shorten the deflagration-to-detonation transition distance. Future work should be carried out and different measurement methods, including the smoke foil and schlieren photographs, will be adopted to explore the detonation-transition mechanism in this micro-combustor.

Acknowledgements. Assistance from Dr. Jian-nan He on experiment design is gratefully acknowledged.

References

[1] Lee, J.H. *The Detonation Phenomenon*, New York, NY: Cambridge University Press, 2008.
[2] Li, J., Lai, W.H., Chung, K. and Lu, F.K. Experimental study on transmission of an overdriven detonation wave from propane/oxygen to propane/air, *Combust. Flame*, 2008, **154**, pp 331–345.
[3] Wu, M., Burke, M.P., Son, S.F. and Yetter, R.A. Flame acceleration and the transition to detonation of stoichiometric ethylene/oxygen in microscale tubes, *Proc. Combust. Inst.* 2007, **31**, pp 2429–2436.
[4] Nobuyuki, T. and Hayashi, A.K. Numerical study on spinning detonations, *Proc. Combust. Inst.*, 2007, **31**, pp 2389–2396.
[5] Bondar, A.Y., Trotsyuk, A.V. and Mikhail, S.I. DSMC Modeling of the detonation wave structure in narrow channels, Orlando, Florida, AIAA 2009-1568, 2009.
[6] Kitano, S., Fukao, M., Susa, A., Tsuboi, N., Hayashi, A.K. and Koshi, M. Spinning detonation and velocity deficit in small diameter tubes, *Proc. Combust. Inst.*, 2009, **32**, pp 2355–2362.
[7] Fischer, J., Liebner, C., Hieronymus, H. and Klemma, E. Maximum safe diameters of microcapillaries for a stoichiometric ethane/oxygen mixture, *Chem. Eng. Sci.*, 2009, **64**, pp 2951–2956.
[8] Camargo, A., Ng, H.D., Chao, J. and Lee, J.H. Propagation of near-limit gaseous detonations in small diameter tubes, *Shock Waves*, 2010, **20**, pp 499–508.
[9] Ishii, K. and Monwar, M. Detonation propagation with velocity deficits in narrow channels, Proc. Combust. Inst., 2011, 33, pp 2359–2366.
[10] Massa, L., Chauhan, M. and Lu, F.K. Detonation-turbulence interaction, *Combust. Flame*, 2011, **158**, pp 1788–1806.
[11] Wu, M.H. and Kuo, W.C. Transmission of near-limit detonation wave through a planar sudden expansion in a narrow channel, *Combust. Flame*, 2012, **159**, pp 3414–3422.

https://doi.org/10.1017/aer.2024.99 Published online by Cambridge University Press

[12] Gao, Y., Ng, H.D. and Lee, J.H. Minimum tube diameters for steady propagation of gaseous detonations, *Shock Waves*, 2014, **24**, pp 447–454.
[13] Starr, A., Lee, J.H. and Ng, H.D. Detonation limits in rough walled tubes, Proc. Combust. Inst., 2015, 35, pp 1989–1996.
[14] Hsu, Y.C., Chao, Y.C. and Chung, K.M. Flame propagation in CH4/H2/O2 blended mixtures in smooth tubes of millimeter-scale, *Combust. Sci. Technol.*, 2016, **188,** (8), pp 1239–1248.
[15] Wang, C., Zhao, Y.Y. and Han, W.H. Effect of heat-Loss boundary on flame acceleration and deflagration-to-detonation transition in narrow channels, *Combust. Sci. Technol.*, 2017, **189,** (9), pp 1605–1623.
[16] Liebner, C., Fischer, J. and Heinrich, S. Are micro reactors inherently safe? An investigation of gas phase explosion propagation limits on ethene mixtures, *Process Safety Environ. Prot.*, 2012, **90**, pp 77–82.
[17] Wu, M.H. and Kuo, W.C. Accelerative expansion and DDT of stoichiometric ethylene/oxygen flame rings in micro-gaps, *Proceedings of the Combustion Institute*, 2013, **34**, pp 2017–2024.
[18] Li, J.Z., Zhang, P.G., Yuan, L., Pan, Z.H. and Zhu, Y.J. Flame propagation and detonation initiation distance of ethylene/oxygen in narrow gap, *Appl. Therm. Eng.*, 2017, **110**, pp 1274–1282.
[19] Cross, M. and Ciccarelli, G. DDT and detonation propagation limits in an obstacle filled tube, *J. Loss Prev. Process Indus.*, 2015, **36**, pp 382–388.
[20] Gordon, S. and McBride, B. Computer program for calculation of complex chemical equilibrium compositions and applications, I. analysis, NASA Reference Publication 1311, October 1994.

Cite this article: Gao Y., Yan Y., Wang Z., Yang B. and Hu H. Experimental research on detonation initiation and transition in millimeter-scale planar combustion chambers. *The Aeronautical Journal*, https://doi.org/10.1017/aer.2024.99